How does a rubber plantation affect the spatial variability and temporal stability of throughfall?

Jiaqing Liu, Wenjie Liu, Weixia Li and Huanhuan Zeng

ABSTRACT

In Xishuangbanna, southwest China, the large-scale monoculture rubber plantation replaced the primary tropical forest, which changed the regional hydrology processes and biogeochemical cycles. As throughfall was an important component of the forest ecosystem water input, we researched the spatial variability and temporal stability of throughfall in the rubber plantation. We recorded 30 rainfall events by using 90 rain gauges during 2015–2016. We found a highly significant linear relationship between rainfall and throughfall, and a strong power correlation between the peak 30 min rainfall intensity and throughfall. The coefficient of variation for throughfall was significant and negatively correlated with rainfall and rainfall intensity. We also observed that throughfall had a strong spatial autocorrelation that would decrease during heavy rainfall events. The results indicate that the leaf area index did not have a significant relationship with throughfall. However, the lateral translocation of the throughfall in the canopy significantly affected the spatial distribution of the throughfall. Generally, the lower throughfall positions were close to the nearest rubber trunk, and the higher throughfall positions were mostly below the slope. This study contributes to the knowledge of the spatiotemporal heterogeneity of throughfall and helps elucidate the interception processes in the rubber plantation.

Key words | rainfall characteristics, rubber, spatial distribution, temporal stability, throughfall

Jiaqing Liu
Wenjie Liu (corresponding author)
Weixia Li
Huanhuan Zeng
CAS Key Laboratory of Tropical Forest Ecology,
Xishuangbanna Tropical Botanical Garden, Chinese Academy of Sciences,
Menglun 666303,
China
E-mail: *lwj@xtbg.org.cn*

Jiaqing Liu
Weixia Li
Huanhuan Zeng
University of Chinese Academy of Sciences,
Beijing 100094,
China

INTRODUCTION

Throughfall (TF) is known as an important component of rainfall partitioning in forest ecosystems; it reaches to the forest floor and affects the eco-hydrology processes and biogeochemical cycles in forested watersheds (Levia & Frost 2006). In addition, many results have confirmed that TF has apparently spatial and temporal variations (e.g. Keim *et al.* 2005; Staelens *et al.* 2006; Zimmermann *et al.* 2007; Kowalska *et al.* 2016). Moreover, this variability can influence the heterogeneity of both soil physicochemical properties, such as soil moisture content (Raat *et al.* 2002), soil solution composition (Návar *et al.* 2009), and the soil microbial community (Rosier *et al.* 2015), and plant physiological processes, such as roots (Li *et al.* 2013), vegetation composition of the underground (Möttönen *et al.* 1999) and nutrient cycling (Laclau *et al.* 2003) in forest ecosystems. This variability also has an effect on localized hydrological processes, such as groundwater recharge (Guswa & Spence 2012), surface runoff and splash erosion (Vega *et al.* 2005; Nanko *et al.* 2010). Therefore, research on the spatial variability and temporal stability of TF is necessary for improving the understanding of forest hydrological and biogeochemical cycling processes and forest ecosystems water management (Levia *et al.* 2011).

In the past decades, many studies on the spatial variability of TF have been conducted in different regions, under different rainfall conditions and below different forest

doi: 10.2166/nh.2018.028

types (Gómez *et al.* 2002; Keim *et al.* 2005; Staelens *et al.* 2006; Zimmermann *et al.* 2007; Shachnovich *et al.* 2008; Zhang *et al.* 2016). The variability of TF has been reported to be influenced by climatic conditions, such as gross rainfall, rainfall intensity and wind direction and speed (Gómez *et al.* 2002; Fan *et al.* 2015; Tanaka *et al.* 2015); and by forest stand factors, such as canopy architecture (Levia & Frost 2006). However, due to the diversity of tree species and various geographic locations with complicated meteorological conditions, previous studies on the spatial variability of TF found inconsistent relationships. For example, Sun *et al.* (2015) found that the spatial patterns of TF were highly related to gross rainfall and did not have a significant relationship with canopy cover or the distance to the nearest trunk in a Japanese cypress plantation. Wullaert *et al.* (2009) demonstrated that excluding the canopy influence, meteorological factors had no significant effect on the spatial variability of throughfall. Zimmermann *et al.* (2010) commented and considered that the combination of rainfall and canopies affected the spatial variability of TF. Additionally, there is little consideration of the spatial variability of the TF in artificial forests and for associated controlling factors in tropical plantation ecosystems.

In Xishuangbanna (Yunnan Province, southwest China), the substantial expansion of rubber plantations replaced the primary tropical forest and induced excessive water loss and soil erosion (Liu *et al.* 2015). The rubber monoculture plantation canopy has changed the redistribution of rainfall to the ground. With daily trampling from latex tapping, the spraying of herbicides and rapid litter decomposition, the surface of the rubber forest became bare. Therefore, splash erosion caused by throughfall is the main focus of soil conservation. In addition, the spatial distribution of TF in the rubber plantation is important for understanding soil erosion and the distribution of soil nutrients in this region; however, there have not been systematic studies on this topic so far (Liu *et al.* 2018). As an irreplaceable economic tree species, there is a clear need for the improved knowledge of key factors contributing to soil erosion in this area. Thus, evaluating the spatial variability and temporal stability of the TF is essential for understanding potential soil water dynamics in artificial forest ecosystems. This will promote the understanding of interception processes in the rubber canopy. Such studies may provide implications for management strategies for soil protection in rubber plantations.

In this study, we focused on the spatial variability and temporal stability of the TF in a rubber plantation. Specifically, the objectives were to: (1) evaluate the effects of canopy structure and rainfall characteristics on the TF variability, (2) describe the spatial distribution of the TF under the rubber canopy, and (3) identify spatial heterogeneities and temporal stability patterns of the TF.

MATERIAL AND METHODS

Study area

The study site was located in the Xishuangbanna Tropical Botanical Gardens (XTBG, 21°55′39″ N, 101°15′55″ E) in the Yunnan Province in southwest China. The rubber plantation was established on a small catchment (19.3 ha), where logging of the tropical rainforest began in 1989. The elevation of the small catchment ranges from 550 to 680 m, with an average slope of 15° (Figure 1(a)). The local climate can be divided into two obvious seasons: the rainy season, from May to October, and the dry season, from November to April (Zhang 1988). According to the meteorological record over the past 40 years, the average annual air temperature was 21.7 °C and that the average annual rainfall was 1,487 mm. Most of the precipitation (87%) occurred during the rainy season, and only 13% of precipitation occurred during the dry season (Liu *et al.* 2015). In the rubber plantation, rubber trees were planted at 2 m × 4 m spacing on the bench terraces. There was a 16 m wide gap separating the two rows that did not have understory vegetation (Figure A1, supplementary material, available with the online version of this paper). A 16 m × 22.5 m research plot was established at the centre of the rubber plantation. The plot contained 24 rubber trees. The mean rubber tree height was 17.4 ± 1.5 m above the ground, and the diameter at breast height (DBH) was 21.2 ± 3.1 cm. The canopy openness was approximately 77 ± 11%, and the height of the first branch was 6.5 ± 0.8 m. The canopy thickness was approximately 6.5 ± 0.5 m, and the mean leaf area index (LAI) was 3.9 ± 0.9 (i.e. mean ± SD). Tree height was measured using a measuring pole as the length from stem

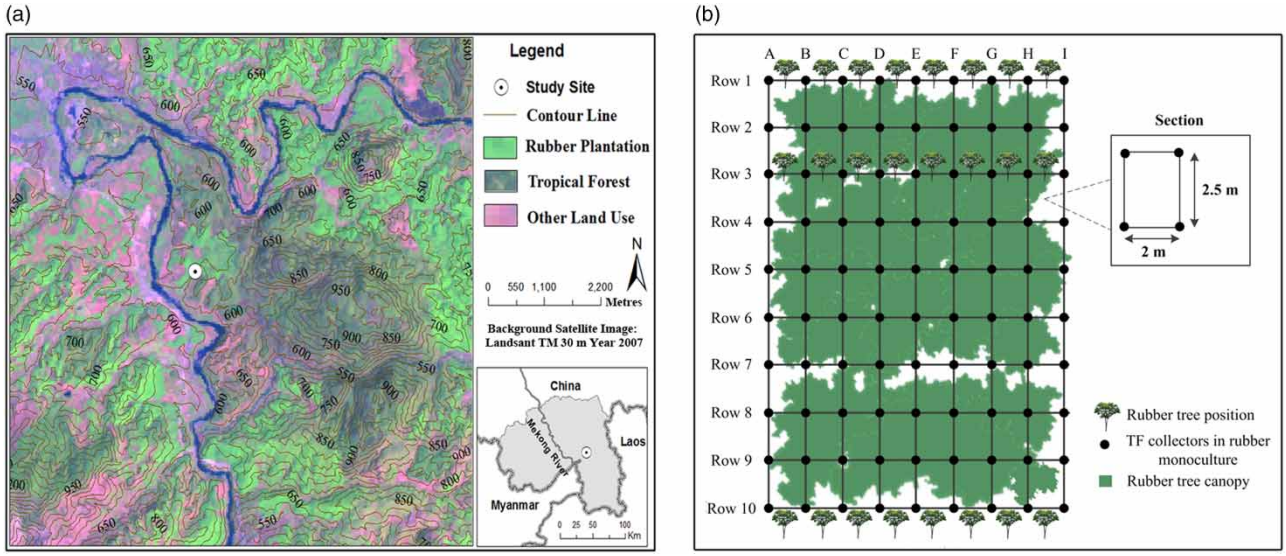

Figure 1 | (a) location of the study site (21°55′39″N, 101°15′55″E) in Yunnan Province, southwest China. (b) Schematic design showing throughfall measurement positions in the field. The green cover is just a schematic of the rubber canopy, which is not based on LAI measurements.

base to apical meristem. DBH was measured using a tapeline and first branch height was measured with tape as the height from the ground to the first branch. The canopy thickness and the canopy openness were visually estimated.

Experimental design

A total of 90 positions were used to measure TF from July 2015 to September 2016. TF was collected using cylindrical plastic rainfall gauges that had collecting areas of 40.15 cm^2. The throughfall collectors can collect a maximum of 500 ml of precipitation and even the strongest rain event during the measuring period did not exceed this. The experimental plot was divided into 10 rows (i.e. from Row 1 to Row 10) and 9 ranks (i.e. from A to I), and the TF collectors were formed on 2×2.5 m grids (Figure 1(b)). All TF collectors remained in the same position during the entire experiment, and they were firmly tied to steel bars, which were inserted into the ground vertically. Therefore, the rainfall gauges were level to the ground surface. TF was measured immediately after every rainfall event to reduce evaporation loss. Two different rainfall events had at least 12 h without rainfall. TF volumes were converted to an equivalent depth by dividing by the horizontal cross-sectional area of the rainfall gauges. A tipping-bucket, self-recording rain gauge was installed in the open field with a resolution of 0.2 mm and a tipping time of 10 minutes (3554WD, Spectrum Technologies Inc., USA). The rain gauge in the open field was next to the rubber plantation. Rainfall characteristics are shown in the supplementary material (Table A1, available with the online version of this paper). To evaluate the influence of rainfall characteristics on TF, the maximum 10 min rainfall intensity (I_{10}, mm 10 min^{-1}), maximum 30 min rainfall intensity (I_{30}, mm 30 min^{-1}), maximum 60 min rainfall intensity (I_{60}, mm h^{-1}), antecedent precipitation index (API), 3-day antecedent wetness index (Index 3) and the 7-day antecedent wetness index (Index 7) were all calculated as co-variables. API is defined by $API = \sum_{i=1}^{30} P_i/i$, where P_i is total gross precipitation on the ith day beforehand (Mizugaki *et al.* 2010). Index 3 and Index 7 are the sum of precipitation for the previous three and seven days, respectively (Zimmermann *et al.* 2007). The LAI was measured once a month as the canopy structure. Because the LAI was measured once a month, we selected an appropriate day to measure the LAI and avoid the convection rainfall. These values were determined above every TF position in the late evening by using the LAI-2200 plant canopy analyser with 90° view caps (Li-Cor Inc., USA). We measured the background A value outside the rubber plantation. Then we went into the forest quickly to measure B. The position of the background A value was near the rubber plantation and

we could arrive at the position of the B value in about one minute. This would reduce the sky brightness change.

Statistical analysis and calculations

By reviewing the literature, the spatial variability of TF had a relationship with the rainfall amount (Gómez *et al.* 2002) and the rainfall intensity (Levia & Frost 2006). Therefore, we classified individual rainfall events by the gross rainfall amount into six different categories (i.e. 5 to <15, 15 to <30, 30 to <40, 40 to <50, 50 to <60, and ≥60 mm) and by the peak 30 min rainfall intensity into four different categories (i.e. 0 to <4, 4 to <8, 8 to <20 and ≥20 mm 30 min^{-1}) to analyse the spatial variability of TF. The rainfall event classes were further expressed as Gr 1, Gr 2, Gr 3, Gr 4, Gr 5 and Gr 6 for the six gross rainfall classes and as G_I 1, G_I 2, G_I 3 and G_I 4 for the four rainfall intensity classes. To maintain the minimum variability in the interclass, clustering analysis was used. We used the Hierarchical Cluster with the nearest neighbour method. Squared Euclidean distance was used to calculate the distance between data points and cluster centre points according to equal variance and statistical independence. In each group, we accumulated the TF of all the individual rainfall events. Descriptive statistics including the mean, standard error of the mean, coefficient of variation (CV, the standard deviation as a proportion of the mean), skewness, and kurtosis were calculated for all groups (Table 1). In addition, the Spearman rank correlation coefficient (rs) was calculated with different cumulative TF classifications.

To describe the temporal stability of TF, TF was normalized by using the following equation which has been used by many authors (Keim *et al.* 2005; Fang *et al.* 2015; Zhang *et al.* 2016):

$$\tilde{T}_{ij} = \frac{T_{ij} - \bar{T}_j}{SD_j} \quad (1)$$

where $\tilde{T}_{ij}$ is the normalized TF at sampling point i for event j, T_{ij} is the TF at sampling point i for event j, and T_j and SD_j are the mean TF and the standard deviation of the TF during that rainfall event, respectively. The normalized TF was arranged from the minimum to the maximum. This type of graph explained two types of temporal stability. First, the extreme persistence was defined as the deviation of the normalized mean TF in the lower and upper quartiles of the arranged positions. Second, the general persistence was defined as the deviation of the normalized mean TF in the interquartile range (Keim *et al.* 2005).

Table 1 | Cumulative throughfall (TF), and median spatial variation coefficient (CV) per rainfall class for 30 events during rainy season of 2015–2016

			TF			
Precipitation class		**No. of events**	**Mean ± SD (mm, $n = 90$)**	**CV (%)**	**Skewness**	**Kurtosis**
	Rainfall (mm)					
Gr 1	5–15	6	38.85 ± 4.14	10.67	–0.70	0.69
Gr 2	15–30	9	155.38 ± 16.88	10.86	–0.36	0.47
Gr 3	30–40	3	80.77 ± 8.50	10.53	–0.08	–0.48
Gr 4	40–50	5	169.95 ± 18.70	11.00	–0.12	0.75
Gr 5	50–60	3	151.82 ± 15.75	10.37	0.23	0.64
Gr 6	>60	4	312.77 ± 23.73	7.59	–0.27	0.07
	I_{30} (mm 30 min^{-1})					
G_I 1	0–4	5	54.50 ± 6.73	12.34	–0.03	0.00
G_I 2	4–8	12	253.52 ± 26.17	10.32	–0.22	0.07
G_I 3	8–20	6	221.40 ± 18.45	8.33	–0.40	0.37
G_I 4	>20	7	380.11 ± 33.80	8.89	–0.02	0.21

Gr, groups of rainfall, G_I, groups of I_{30}.

Semivariogram analysis is an important method for reflecting spatial variability. This analysis expresses spatial autocorrelation at different positions. To analyse the spatial characteristics of TF, we also calculate the semivariogram $\gamma(h)$. The model is as follows:

$$\gamma(h) = \frac{1}{2n(h)} \sum_{i=1}^{n(h)} [Z(x_i) - Z(x_{i+h})]^2 \quad (2)$$

where $n(h)$ is the number of sample pairs at each distance interval h, and $Z(x_i)$ and $Z(x_i + h)$ are the values of the variable at any two positions that are separated by a lag distance h. The experimental variogram is calculated for several lag distances. The lag h is defined as a vector with both distance and direction. An appropriate semivariogram for the cumulative TF is computed by adjusting active lag distances until the minimum residual sum of squares (*RSS*) and the predicted maximum coefficient of determination (R^2) are both obtained. The parameters of the model include the model type, nugget (C_0), sill ($C + C_0$), Partial Sill (C), Partial Sill/Sill and fractural D. If the Partial Sill/Sill was larger than 75%, this indicated a strong spatial autocorrelation. If the Partial Sill/Sill was smaller than 25%, this indicated a weak spatial autocorrelation. If the Partial Sill/Sill was between 25% and 75%, this indicated a moderate spatial autocorrelation. Fractural D indicated the change of throughfall in a different direction.

The contour maps in this paper were drawn using Golden Software Surfer 10 (Golden Software Inc.) based on a kriging interpolation. The cumulative TF in different categories are calculated with GS$^+$ 9.0 (Gamma Design Software) for semivariograms analysis. All other statistical analyses were conducted using IBM SPSS statistics 22.0 (IBM Inc.). The normality of the TF was tested using the Kolmogorov-Smirnov test. A principal component analysis (PCA) was performed to analyse the effects of rainfall characteristics and canopy traits on TF, including rainfall, LAI, API, Index 3, Index 7, I_{10}, I_{30} and I_{60} during the 30 rainfall events. The PCA was calculated using Canoco version 4.5. The relationship between rainfall characteristics and throughfall was determined using the linear and the power functions, and the coefficient of determination was used. The lateral translocation of the throughfall in tree crowns is an important parameter of the canopy water redistribution. To analyse the lateral flow of the tree canopy, we calculated the parameter c of each sample point. First, we analysed scatterplots of throughfall and gross rainfall to find a value for the saturation of canopy storage capacity, and we found the gross rainfall exceeded this in all 30 rainfall events. Then we used the following equation to calculate the parameter c (Frischbier & Wagner 2015):

$$TF = c\mathrm{GR} + \varepsilon \quad (3)$$

where c is an additional parameter which describes the relationship between lateral flow and gross rainfall (GR). ε is an error term. If $c < 1$, then a lateral water discharge flow occurred, and if $c > 1$, then a lateral water inflow occurred. For further information regarding this theory and calibration, see Frischbier & Wagner (2015).

RESULTS

Throughfall and rainfall characteristics

Between July 2015 and September 2016, a total of 1,112.9 mm of rainfall was collected from 30 individual rainfall events; 13 rainfall events occurred in July, 11 rainfall events occurred in August and six rainfall events occurred in September. The gross rainfall ranged from 6.5 mm to 108.4 mm. Other rainfall characteristics for each event in the rubber plantation are provided in Table A1 (available with the online version of this paper). Cumulative TF was 909.5 mm with an 81.7% average (SD = 10.1%). For all events, we found a strong linear correlation ($P < 0.01$) between gross rainfall (RG) and TF for each event (Figure 2(a)), and there was also a strong power correlation ($P < 0.01$) between the maximum 30 min rainfall intensity and TF (Figure 2(b)). The coefficients of variation for TF (CV_{TF}) were calculated using data for each event. CV_{TF} ranged from 8.56% to 22.87%, with a 15.03% average and decreased with increasing gross rainfall (Figure 2(c)) and I_{30} (Figure 2(d)). There was a strong linear correlation ($P < 0.01$) between the gross rainfall and CV_{TF} for each event, and there was also a strong power correlation ($P < 0.01$) between I_{30} and CV_{TF}. The TF ratio ranged from 60.75% to

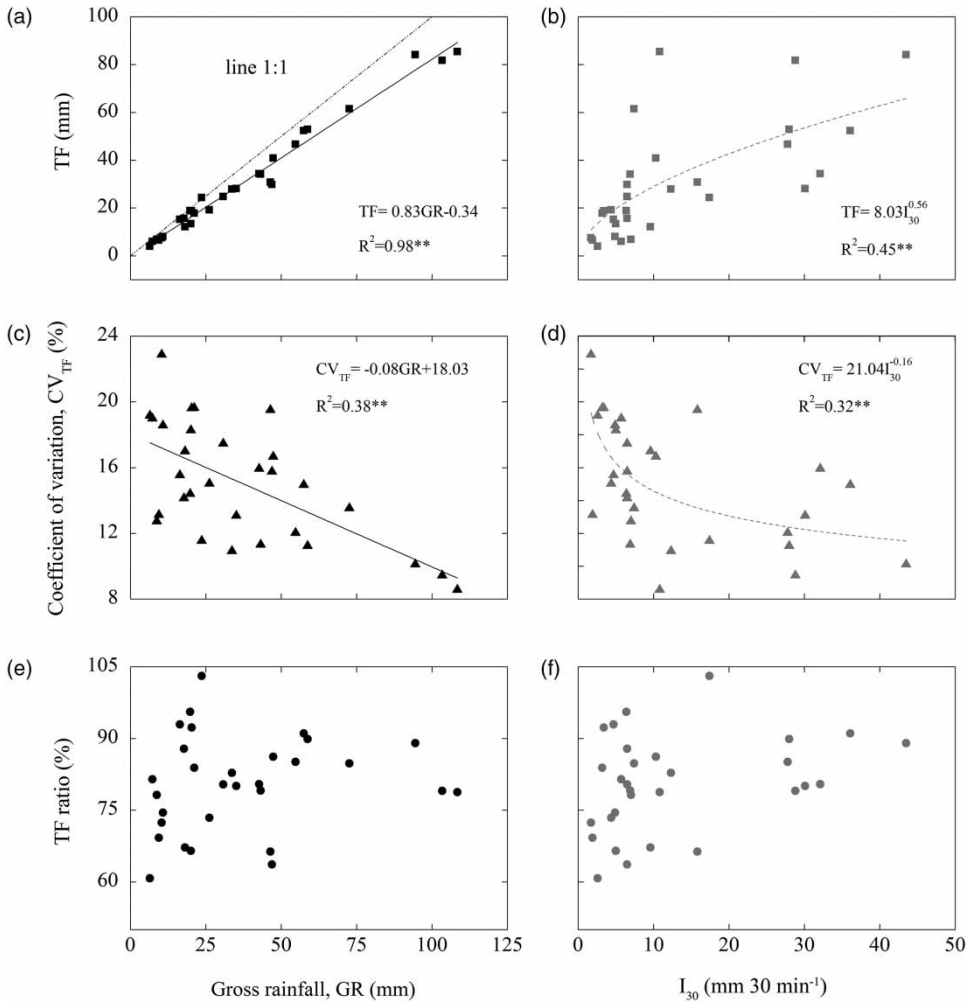

Figure 2 | (a) Throughfall (TF) plotted against gross rainfall (GR) and (b) peak 30 min rainfall intensity (I_{30}) to determine the canopy interception capacity for the rubber monoculture plantation. (c) The relationship between the gross rainfall and the coefficient of variation for throughfall (CV_{TF}). (d) The relationship between I_{30} and the CV_{TF}. (e) The relationship between the gross rainfall and the throughfall ratio (TF ratio). (f) The relationship between I_{30} and the TF ratio. $^{**}P < 0.01$.

103.06% and increased at first with gross rainfall less than 25 mm. When the gross rainfall was more than 25 mm, the TF ratio trended to be stabilized while gross rainfall increased (Figure 2(e)). Furthermore, the TF ratio also had a large fluctuation when the I_{30} was less than 8 mm 30 min^{-1}. In addition, it was nearly stable when I_{30} was >8 mm 30 min^{-1} (Figure 2(f)). To describe the integrated effects of the rainfall characteristics (i.e. gross rainfall, I_{10}, I_{30}, I_{60}, Index 3, Index 7 and API) in response to TF, a principal component analysis of the rainfall parameters was performed (Figure 3). The PCA showed significant effects of the rainfall amount and the rainfall intensity on TF. The first axis of the PCA explained 59.2% of the variance in the TF data, and the second axis explained 25.9% of the variance. The TF under the rubber monoculture plantation was strongly affected by the rainfall characteristics, especially gross rainfall. The TF was less affected by the antecedent rainfall parameters.

Spatial heterogeneity of throughfall under the canopy

The coefficients of variation for the cumulative TF ranged from 7.59% to 11.00% in the rainfall classification and from 8.33% to 12.34% in the rainfall intensity classification (Table 1). Moreover, we used geostatistical methods to analyse the spatial differences of the cumulative TF. Table 2 summarizes the semivariance parameters of the two

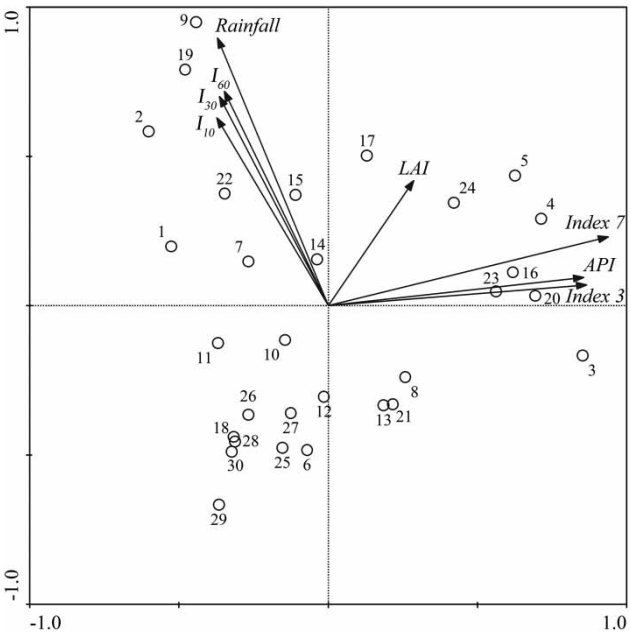

Figure 3 | Correlation biplot based on a PCA of the rainfall characteristics and leaf area index (LAI) in the rubber monoculture plantation. The eigenvalues of the first four axes are 0.592, 0.259, 0.076, and 0.055, respectively. Hollow circles represent all 30 rainfall events. I_{10} (mm 10 min^{-1}), I_{30} (mm 30 min^{-1}) and I_{60} (mm h^{-1}) are the maximum 10, 30 and 60 min rainfall intensities, respectively. API is antecedent precipitation index. Index 3 and Index 7 are the 3- and 7-day antecedent wetness indices, respectively.

different classifications. In the gross rainfall classification, the Partial Sill/Sill for the first five groups was in the range of 82.9–88.6%, belonging to the strong spatial autocorrelation category (>75%). However, in the Gr 6 group, the value was 55.5%. In Gr 6, there were four rainfall events recorded, and the gross rainfall of each event was >60 mm. The heavy gross rainfall may be a result of moderate spatial autocorrelation. In the rainfall intensity classification, the values of the Partial Sill/Sill for G_I 1 and G_I 2 were 84.7% and 85.3%, respectively. They also belonged to the strong spatial autocorrelation category. However, in the G_I 3 and G_I 4 groups, there was also a moderate amount of spatial autocorrelation. This may be because of the rainfall intensity. A maximum 30 min rainfall intensity that was more than 8 mm 30 min^{-1} caused moderate spatial autocorrelation. The fractural D of the TF was not significantly different in each direction for different rainfall and rainfall intensities, indicating that the degree of spatial heterogeneity was stable under the entire rubber canopy (Figure 4(a) and 4(b)). The sill ($C_0 + C$) represents the largest variation in the regionalized variables. The sill of the TF percentage of rainfall decreased with an increase in rainfall (Figure 4(c)). Furthermore, the sill had large fluctuations when I_{30} was less than 8 mm 30 min^{-1} and was nearly stable when I_{30} was more than 8 mm 30 min^{-1} (Figure 4(d)).

Spatial distribution of throughfall under the canopy

There was no significant correlation between the TF and the LAI in all the rainfall events in the same position with raw measurements from different months ($P > 0.05$). However, there was a significant correlation between the TF and the parameter c ($R^2 = 0.868$, $P < 0.01$), which exhibited similar trends in each row (Figure 5). In addition, the parameter c

Table 2 | Parameters of semivariogram models for the cumulative throughfall in different groups

Event	Theoretical model	Nugget	Sill	R^2	RSS*	$C/(C_0+C)$
Gr 1	Exp	0.00188	0.01386	0.860	1.14×10^{-06}	0.864
Gr 2	Exp	0.00219	0.01428	0.987	1.38×10^{-07}	0.847
Gr 3	Exp	0.00159	0.01238	0.751	5.26×10^{-07}	0.872
Gr 4	Exp	0.00247	0.01444	0.769	3.12×10^{-06}	0.829
Gr 5	Exp	0.00131	0.01152	0.842	1.09×10^{-06}	0.886
Gr 6	Exp	0.00319	0.00717	0.926	2.32×10^{-07}	0.555
G_I 1	Exp	0.00269	0.01758	0.848	2.12×10^{-06}	0.847
G_I 2	Exp	0.00183	0.01246	0.959	3.26×10^{-07}	0.853
G_I 3	Exp	0.00514	0.01029	0.985	5.60×10^{-08}	0.500
G_I 4	Exp	0.00463	0.00963	0.909	4.64×10^{-07}	0.519

Exp, exponential theoretical variogram model. *Residual sums of squares that provide a measure of how well the model fits the variogram data. Gr, groups of rainfall, G_I, groups of I_{30}.

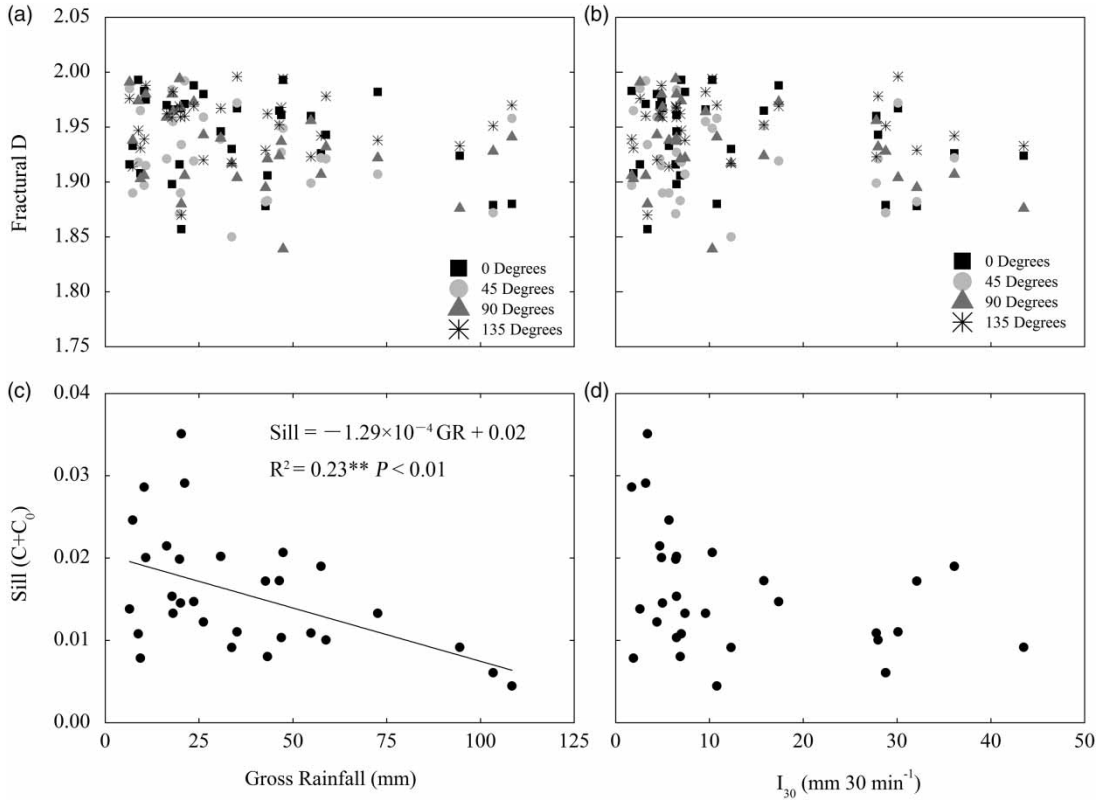

Figure 4 | Change of fractural D of throughfall with rainfall (a) and I_{30} (b). Change of the sill ($C + C_0$) of throughfall ratio with rainfall (c) and I_{30} (d). The sill refers to the maximum variance of throughfall in different rainfall events.

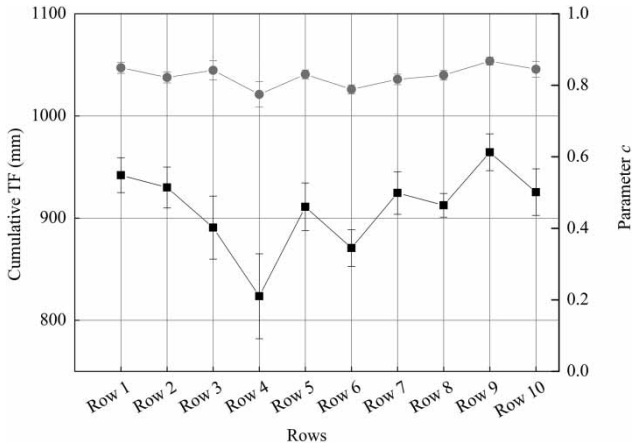

Figure 5 | The cumulative throughfall and the parameter c of the lateral translocation of the throughfall in different rows.

was all smaller than 1 at each position. The canopy interception effectively affected the spatial distribution of TF, but the LAI had no obvious relationship with the spatial distribution of TF. The cumulative TF showed some differences in gross rainfall classifications for each group (Figure 6). In every group, a belt with low TF appeared from Row 3 to Row 5. This belt was close to the nearest rubber trunk. The belt with low TF became larger as rainfall increased from Gr 1 to Gr 3. When the rainfall amount ranged from 50 to 60 mm (Gr 4), the spatial distribution of TF was the most homogeneous in the plot. The spatial distribution of TF in Gr 4 and Gr 6 was similar, and showed large variability. The results indicated that the spatial distribution of TF was more even and homogeneous when the rainfall amount ranged from 5 to 40 mm. The 40 mm rainfall was used as a threshold that affected the spatial distribution of TF. The spatial distribution of the cumulative TF was also different in the different groups depending on rainfall intensity (Figure 7). In every group, a belt with a low TF also appeared from Row 3 to Row 5, which was close to the nearest rubber trunk. From G_I 1 to G_I 3, with the rainfall intensity increasing, the spatial distribution of low TF decreased. In G_I 4, low TF was largest, indicating that when the maximum 30 min

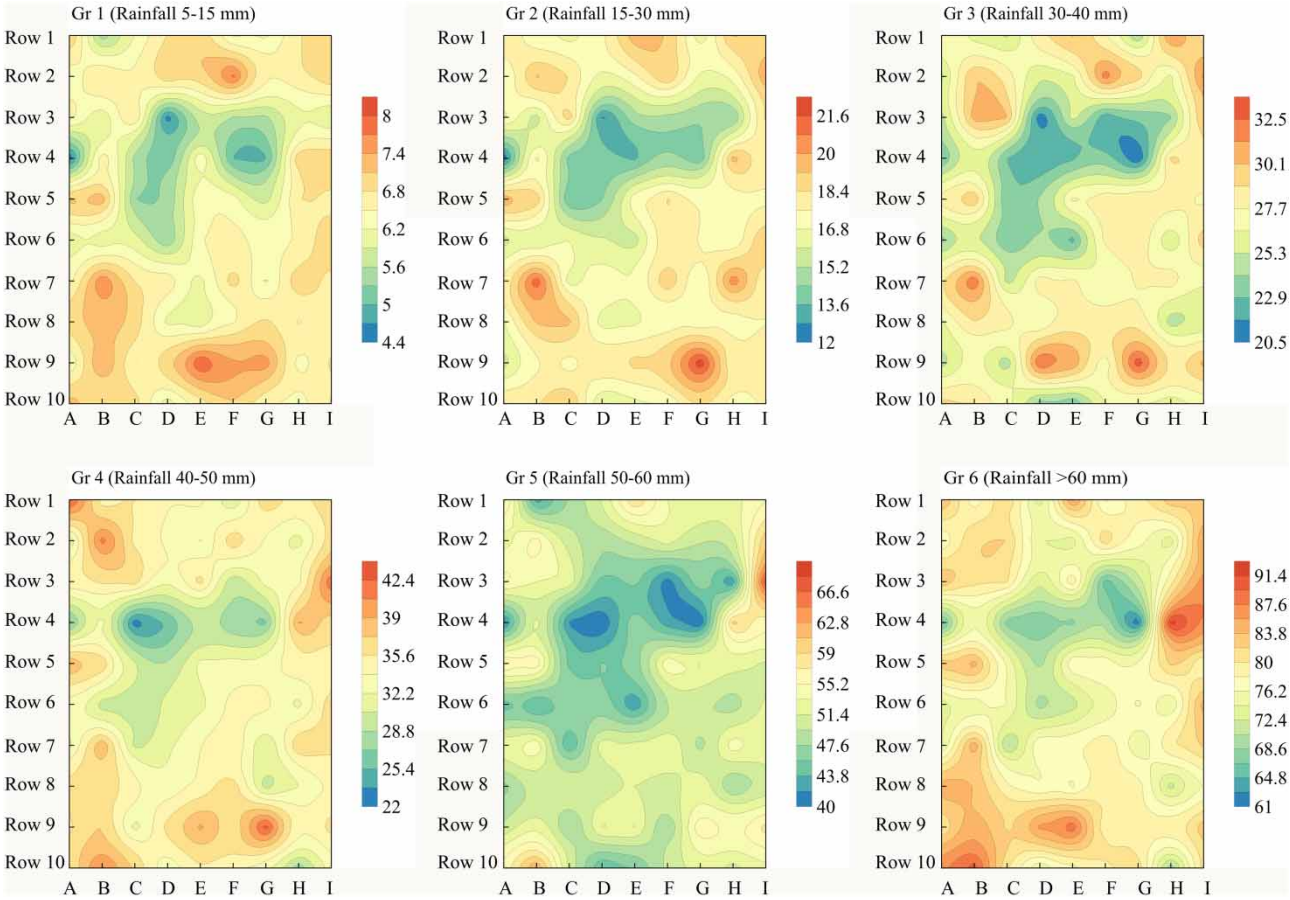

Figure 6 | Spatial distribution of the cumulative throughfall of different gross rainfall groups in the rubber monoculture plantation. Gr 1, Gr 2, Gr 3, Gr 4, Gr 5 and Gr 6 represent Group 1, Group 2, Group 3, Group 4, Group 5 and Group 6, respectively.

rainfall intensity was more than 20 mm 30 min^{-1}, the spatial distribution of TF was more even and homogeneous.

Temporal persistence of throughfall

The Spearman correlation analysis showed significant positive results ($P < 0.01$) in six rainfall classes and four rainfall intensity classes (Table 3). In this regard, we calculated the cumulative TF for 30 rainfall events to analyse the temporal stability of spatial TF. Figure 8 shows temporal stability plots for mean TF in each collector position and for different rows. The temporal stability of spatial TF was stable with a moderate general persistence under the rubber plantation. The mean normalized TF was significantly different than zero for only 1.6% of the samples (t-test; $a = 0.05$). The temporal stability of TF in different rows was also stable and revealed a consistent distribution of TF with the counter map. Only a few collector positions were extremely wet and extremely dry. For example, 9G was in Row 9 and 4A and 4D were in Row 4. The dry positions were mostly in Row 4, and the wet positions were likely near to Row 9.

DISCUSSION

Effects of rainfall characteristics on throughfall

The relationship between TF and gross rainfall has already been studied in many countries and regions, and most of the results confirmed that there was a strong and significant linear correlation between the two (Kato *et al.* 2013; Zhang *et al.* 2016). Our results were also consistent with these studies. However, there was no consensus regarding the relationship between TF and rainfall intensity. In the

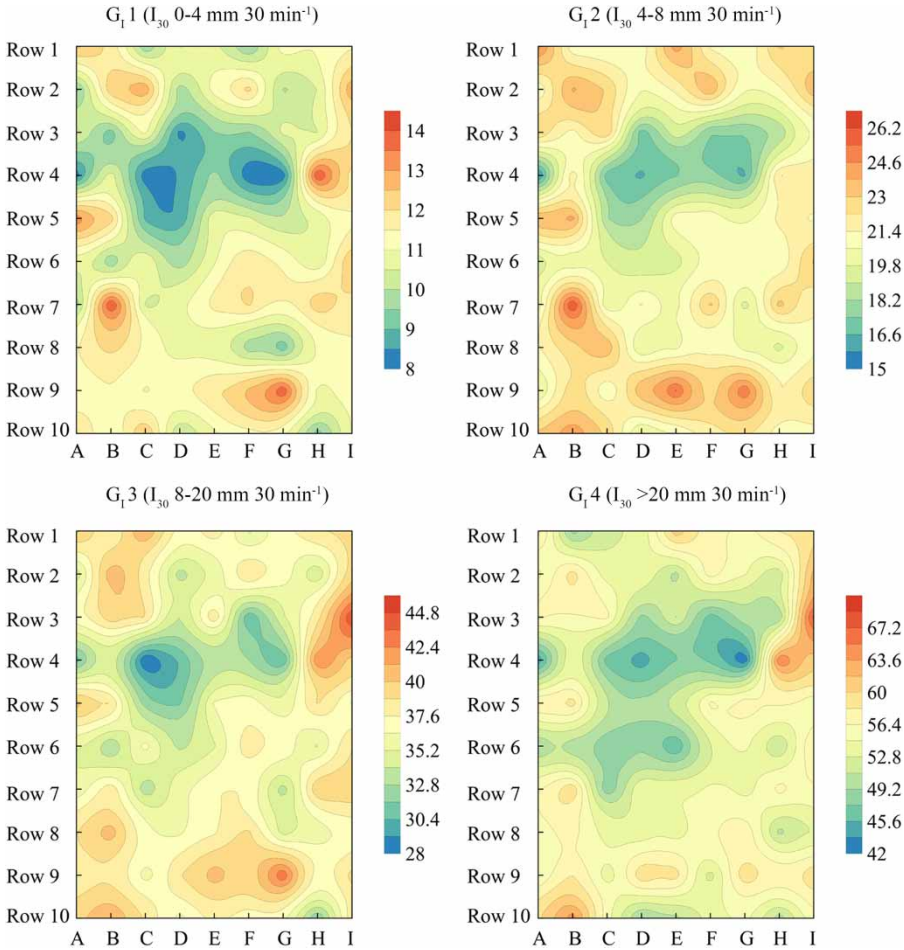

Figure 7 | Spatial distribution of the cumulative throughfall of different peak 30 min rainfall intensity groups in the rubber monoculture plantation. G_I 1, G_I 2, G_I 3 and G_I 4 represent Group 1, Group 2, Group 3 and Group 4, respectively.

Table 3 | Spearman rank correlation coefficients ($n = 90$) between the cumulative throughfall (TF) of rain events within different rainfall classes

	Summed TF with rainfall class (mm)					**Summed TF with I_{30} class (mm 30 min^{-1})**			
	15 –< 30	**30 –< 40**	**40 –< 50**	**50 –< 60**	**≥ 60**		**4 –< 8**	**8 –< 20**	**≥ 20**
5 –< 15	0.761**	0.618**	0.642**	0.599**	0.655**	0 –< 4	0.736**	0.716**	0.594**
15 –< 30		0.774**	0.663**	0.777**	0.684**	4 –< 8		0.723**	0.789**
30 –< 40			0.659**	0.786**	0.687**	8 –< 20			0.746**
40 –< 50				0.673**	0.828**				
50 –< 60					0.735**				

**$P < 0.01$.

rubber plantation, there was a significant power correlation between TF and I_{30}, which was different from other studies (Levia & Frost 2006; Zhang *et al.* 2016). The reason for this may be due to different types of rainfall in various geographic locations. Therefore, both rainfall and rainfall intensity (i.e. I_{30}) were important indicators for the evaluation of water input in the tropical rubber plantation forest floor. In addition, we found there was a significant linear

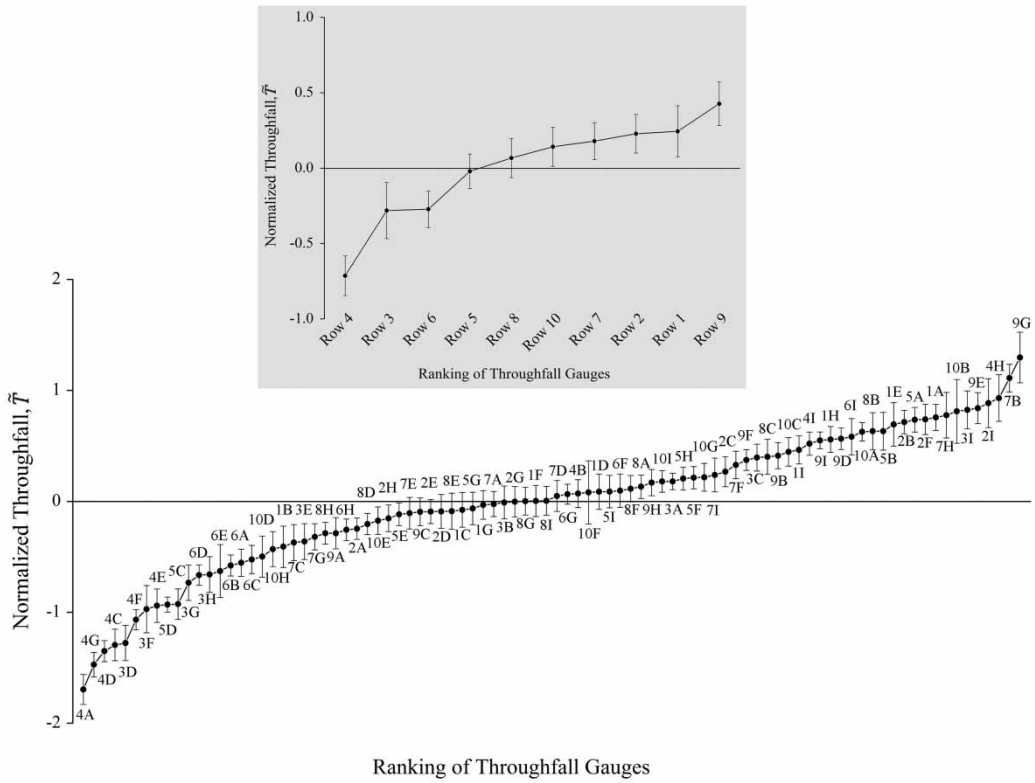

Figure 8 | Time stability plots of throughfall water normalized to zero mean and unit variance. The collectors are plotted along the horizontal axis and ranked by their means, $\tilde{T}$. Error bars represent ± SD. The names in the figure are the rainfall collectors in the plot. The time stability plots of throughfall normalized in each row are shown in the middle of this figure.

positive correlation between throughfall kinetic energy and TF (Liu *et al.* 2018). So rainfall amount may be a critical factor for prediction of soil detachment in rubber plantations, which would provide implications for management strategies for soil protection in this region.

Generally, the TF ratio is an important indicator of the canopy saturation process and how much rainfall would fall to the forest ground (Carlyle-Moses *et al.* 2004). The average value of TF ratio was 82% in this study. This was also similar to other findings in tropical forests (Zimmermann *et al.* 2007; Teale *et al.* 2014). The higher TF percentage in the tropics may be due to the higher rainfall intensity, producing larger raindrops (Levia *et al.* 2017). When the rainfall is small or rainfall intensity is low, most of the rainfall is first intercepted by the canopy; as the rainfall or rainfall intensity exceeds a certain threshold, the canopy saturates quickly and generates a great deal of free throughfall, which helps make the TF ratio stable. In this study, we did not compare the TF between the rubber plantation and rainforest in this region, as the rainforest is a little far away from the rubber plantation and there were some differences in rainfall characteristics and geological properties. Sometimes, it was raining in the rubber plantation but in the rainforest it was not. Therefore it was not appropriate to compare TF for a rainfall event. We will conduct long observation periods (such as weekly periods) to analyse the spatial distribution differences of TF between rainforest and artificial forest in future studies.

The CV_{TF} has been reported in numerous studies (Shen *et al.* 2012; Kato *et al.* 2013; Zhang *et al.* 2016). The average CV_{TF} (15%) in this study plot for the rubber plantation was lower and more stable than that in most studies. Kato *et al.* (2013) reported that the CV_{TF} was 52% (from 10% to 447%) in a Japanese cypress plantation, and Shen *et al.* (2012) found that CV_{TF} ranged from 25% to 39% in an evergreen broad-leaved forest in eastern China. With different forest types, meteorological conditions and experimental designs, it was difficult to compare our results with earlier

studies. Nevertheless, a relationship between rainfall characteristics and CV_{TF} was likely under different conditions. Most studies confirmed that the CV_{TF} decreased with an increase in rainfall (Loustau *et al.* 1992; Teale *et al.* 2014; Fan *et al.* 2015; Zhang *et al.* 2016). In many studies, the relationship between rainfall and CV_{TF} was a power function (Shen *et al.* 2012; Kato *et al.* 2013; Zhang *et al.* 2016). However, a linear regression was more suitable in this study, and similar results were found in other tropical places (Teale *et al.* 2014; Fan *et al.* 2015). Currently, the effect of rainfall intensity on CV_{TF} has been investigated in few studies. Some studies found that there was significant negative correlation, following power functions, between rainfall intensity and CV_{TF} (Fan *et al.* 2015; Zhang *et al.* 2016), which was consistent with our result. The key reason for this was the process of canopy interactions and saturation. When rainfall was small, canopy interception led to a large variability in TF; when rainfall was heavy, a rapidly saturated canopy produced free TF (Carlyle-Moses *et al.* 2004). The PCA analysis also confirmed that rainfall and rainfall intensity were the main factors affecting the TF. However, the effect of antecedent rainfall index on TF was weak, possibly due to the rainfall in the canopy evaporating very quickly and the antecedent canopy wetness does not have a significant impact on TF.

The spatial heterogeneity and temporal stability of throughfall

In this study, we found that both rainfall and rainfall intensity have a significant correlation with TF, so we classified rainfall and I_{30} into different categories to analyse the spatial distribution of the TF. The structure of the spatial variability of TF showed that spatial variations relied on a suitable distance. TF under the rubber plantation was spatially autocorrelated at a range of approximately 4–6 m and had a meaningful nugget effect for the gross rainfall classification (except for Gr 6). In Gr 6, the gross rainfall from each rainfall event was more than 60 mm, and both rainfall ratios and CV_{TF} values were fairly conservative. More random factors affected the spatial heterogeneity of Gr 6, creating a moderate spatial autocorrelation. Furthermore, in the rainfall intensity classification, when I_{30} was more than 8 mm 30 min^{-1}, the spatial autocorrelation also became moderate.

Some studies regarding the spatial correlation of TF had different results. Some studies have shown that TF had a spatial autocorrelation at a certain distance (Gómez *et al.* 2002; Staelens *et al.* 2006), and other studies found no spatial autocorrelation at different TF sample positions (Loustau *et al.* 1992). These different results may be explained by differences in canopy architecture and meteorological phenomena (Keim *et al.* 2005). A large number of samples were needed to attain spatial variability patterns for TF with low gross rainfall (Zimmermann *et al.* 2010). Moreover, variograms of TF appeared to be unstable and required more calibration and mathematical simulations (Keim *et al.* 2005). The sill of the TF ratio decreased as the gross rainfall increased, indicating that a heavy rainfall event caused the spatial heterogeneity of the TF ratio to be uniform. The fractural D of the TF had no significant change for every direction and was not affected by rainfall or rainfall intensity. The reason for this may be due to the combination of rainfall, wind speed, rainfall intensity and other factors (Shi *et al.* 2006; Fang *et al.* 2015). Therefore, the spatial directionality of TF requires more rainfall events for future studies.

The temporal stability results showed that the TF was generally persistent, and the results were consistent with the low CV_{TF}. Furthermore, some positions in Row 4 exhibited persistent dry conditions. The dry positions may be due to the branches above them; and moss and other epiphytes were attached to the branches, which can store much water and act as a TF shelters. In addition, the wet positions may have been just below the drop tips from the branches and leaves (Zimmermann *et al.* 2007). The summed TF of each rainfall and rainfall intensity class had significant relationships with each other (with the Spearman's rank correlation test), which was consistent with results from different time periods (Staelens *et al.* 2006; Fathizadeh *et al.* 2014; Kowalska *et al.* 2016).

The spatial distribution characteristics of throughfall

Some studies have found that monoculture plantations alter stand structures and play an important role in changing the spatial distribution of TF (Teale *et al.* 2014; Sun *et al.* 2015; Tanaka *et al.* 2015). Many studies have researched the relationship between TF and LAI, which is an important

index of the canopy. In our study, TF had no clear relationship with LAI, which was consistent with previous studies (Teale *et al.* 2014; Kowalska *et al.* 2016). As Fang *et al.* (2015) demonstrated, when the rainfall was low, TF and LAI had a strong linear correlation. However, when the rainfall became heavy, this relationship was weak. In the Xishuangbanna rubber plantation, which had heavy rainfall and strong rainfall intensity, our results suggested that LAI was not sufficient to analyse the canopy effect on TF. However, we confirmed the lateral water translocation in the canopy was important for the spatial distribution of TF.

The spatial distribution patterns of TF were a little different depending on the different rainfall amounts and rainfall intensity classes. Furthermore, the spatial distribution of TF was highly heterogeneous and was not correlated with the distance to the tree trunk. Many studies observed similar results for different types of forests (Loustau *et al.* 1992; Shachnovich *et al.* 2008; Sun *et al.* 2015; Nanko *et al.* 2016). However, the TF was concentrated at certain points, and the same positions were observed for different rainfall and rainfall intensity classes. The lowest concentration of TF was close to the nearest rubber trunk (Row 4). The highest TF positions were primarily below the slope (Row 9). Temporal stability results also supported this result.

The spatial distribution patterns of TF may be explained by the canopy cover (i.e. the branches and leaves) and the wind combined (Carlyle-Moses *et al.* 2004; Keim *et al.* 2005; Staelens *et al.* 2006; Zimmermann *et al.* 2010). The canopy redistributed the rainfall due to the angle of the branches, which determined the drip points (Gerrits *et al.* 2010). Therefore, branches would store more rainfall than leaves (Llorens & Gallart 2000); in addition, the effect of leaves on the distribution of TF decreased sharply when completely wetted (Carlyle-Moses *et al.* 2004). Another reason for the spatial distribution patterns of TF was the angle of the branches; the funnel-shaped branch structure allowed the rainfall to form a stemflow, which reduced the TF below the covered branch positions (Herwitz 1987; Levia & Frost 2006). Close to the nearest rubber trunk, more branches and leaves intercepted the TF, which resulted in a lower value at this position. Wind conditions were also key factors when considering the spatial patterns of TF under the rubber canopy. One reasonable hypothesis is that the slope of the regression line decreases as wind speed increases because the wind-induced vibration of the leaves changes the water flow and storage in the canopy (Hörmann *et al.* 1996; Llorens & Gallart 2000). Additionally, wind alters the incident angles of rainfall and changes the effective interception area, thus changing the amount of rainfall intercepted by the tree crown (Kato *et al.* 2013). This is why the TF was high below the slope. Our results suggested that we need more careful measurements to confirm the biotic and abiotic factors affecting the spatial distribution of TF.

CONCLUSION

In this study, we analysed the spatial variability of TF and its temporal stability in a rubber plantation. Specifically, we evaluated the effect of rainfall characteristics and canopy architecture on the variability of TF and described the spatial distribution of TF. The results indicated that there was a strong linear correlation between gross rainfall and TF for each event and a strong power correlation between peak 30 min rainfall intensity and TF. We also found that CV_{TF} decreased with increasing gross rainfall and rainfall intensity. We also observed that TF had a strong spatial autocorrelation that would decrease during heavy rainfall events. The results indicated that the LAI had no significant influence on the spatial distribution of TF. We interpreted this spatial dependence to be caused by the rainfall drop redistribution, which was caused by rubber leaves and branches, complex meteorological factors, and, in particular, the wind. However, the lateral translocation of the TF in the canopy significantly affected the spatial distribution of the TF. The TF was concentrated at certain similar points in different rainfall and rainfall intensity classes. The lowest TF positions were close to the nearest rubber trunk, and the highest TF positions were mostly below the slope. Temporal stability analyses also confirmed this result. Future studies need to quantify the effect of other factors on the spatial distribution of TF, as well as the spatiotemporal patterns of solute deposition in the rubber plantation. Such studies are essential to help us understand the distribution of soil moisture and nutrients, the water cycle and interception processes in the artificial forest ecosystem.

ACKNOWLEDGEMENTS

We thank Mr Liu MN and the Central Laboratory of XTBG for their help. This study was supported by the National Natural Science Foundation of China (31570622 and 41701029), the Natural Science Foundation of Yunnan Province (2014HB042), and the CAS 135 program (No. 2017XTBG-F01).

COMPETING FINANCIAL INTERESTS

The authors declare no competing financial interests.

REFERENCES

Carlyle-Moses, D., Laureano, J. F. & Price, A. 2004 Throughfall and throughfall spatial variability in Madrean oak forest communities of northeastern Mexico. *Journal of Hydrology* **297** (1), 124–135. DOI: 10.1016/j.jhydrol.2004.04.007.

Fan, J., Oestergaard, K. T., Guyot, A., Jensen, D. G. & Lockington, D. A. 2015 Spatial variability of throughfall and stemflow in an exotic pine plantation of subtropical coastal Australia. *Hydrological Processes* **29** (5), 793–804. DOI: 10.1002/hyp.10193.

Fang, S., Zhao, C. & Jian, S. 2015 Spatial variability of throughfall in a *Pinus tabulaeformis* plantation forest in Loess Plateau, China. *Scandinavian Journal of Forest Research* **31** (5), 467–476. DOI: 10.1080/02827581.2015.1092575.

Fathizadeh, O., Attarod, P., Keim, R. F., Stein, A., Amiri, G. Z. & Darvishsefat, A. A. 2014 Spatial heterogeneity and temporal stability of throughfall under individual *Quercus brantii* trees. *Hydrological Processes* **28** (3), 1124–1136. DOI: 10.1002/hyp.9638.

Frischbier, N. & Wagner, S. 2015 Detection, quantification and modelling of small-scale lateral translocation of throughfall in tree crowns of European beech (*Fagus sylvatica* L.) and Norway spruce (*Picea abies* (L.) Karst.). *Journal of Hydrology* **522**, 228–238. DOI: 10.1016/j.jhydrol.2014.12.034.

Gerrits, A., Pfister, L. & Savenije, H. 2010 Spatial and temporal variability of canopy and forest floor interception in a beech forest. *Hydrological Processes* **24** (21), 3011–3025. DOI: 10.1002/hyp.7712.

Gómez, J., Vanderlinden, K., Giráldez, J. & Fereres, E. 2002 Rainfall concentration under olive trees. *Agricultural Water Management* **55** (1), 53–70. DOI: 10.1016/S0378-3774(01)00181-0.

Guswa, A. J. & Spence, C. M. 2012 Effect of throughfall variability on recharge: application to hemlock and deciduous forests in western Massachusetts. *Ecohydrology* **5** (5), 563–574. DOI: 10.1002/eco.281.

Herwitz, S. R. 1987 Raindrop impact and water flow on the vegetative surfaces of trees and the effects on stemflow and throughfall generation. *Earth Surface Processes and Landforms* **12** (4), 425–432. DOI: 10.1002/esp.3290120408.

Hörmann, G., Branding, A., Clemen, T., Herbst, M., Hinrichs, A. & Thamm, F. 1996 Calculation and simulation of wind controlled canopy interception of a beech forest in Northern Germany. *Agricultural and Forest Meteorology* **79** (3), 131–148. DOI: 10.1016/0168-1923(95)02275-9.

Kato, H., Onda, Y., Kazuki, N., Gomi, T., Yamanaka, T. & Kawaguchi, S. 2013 Effect of canopy interception on spatial variability and isotopic composition of throughfall in Japanese cypress plantations. *Journal of Hydrology* **504**, 1–11. DOI: 10.1016/j.jhydrol.2013.09.028.

Keim, R. F., Skaugset, A. E. & Weiler, M. 2005 Temporal persistence of spatial patterns in throughfall. *Journal of Hydrology* **314** (1), 263–274. DOI: 10.1016/j.jhydrol.2005.03.021.

Kowalska, A., Boczoń, A., Hildebrand, R. & Polkowska, Ż. 2016 Spatial variability of throughfall in a stand of Scots pine (*Pinus sylvestris* L.) with deciduous admixture as influenced by canopy cover and stem distance. *Journal of Hydrology* **538**, 231–242. DOI: 10.1016/j.jhydrol.2016.04.023.

Laclau, J. P., Ranger, J., Bouillet, J. P., de Dieu Nzila, J. & Deleporte, P. 2003 Nutrient cycling in a clonal stand of *Eucalyptus* and an adjacent savanna ecosystem in Congo: 1. Chemical composition of rainfall, throughfall and stemflow solutions. *Forest Ecology and Management* **176** (1), 105–119. DOI: 10.1016/S0378-1127(02)00280-3.

Levia Jr, D. F. & Frost, E. E. 2006 Variability of throughfall volume and solute inputs in wooded ecosystems. *Progress in Physical Geography* **30** (5), 605–632. DOI: 10.1177/0309133306071145.

Levia, D. F., Keim, R. F., Carlyle-Moses, D. E. & Frost, E. E. 2011 Throughfall and stemflow in wooded ecosystems. In: *Forest Hydrology and Biogeochemistry* (D. F. Levia, D. Carlyle-Moses & T. Tanaka, eds). Springer, Berlin, pp. 425–443. DOI:10.1007/978-94-007-1363-5_21.

Levia, D. F., Hudson, S. A., Llorens, P. & Nanko, K. 2017 Throughfall drop size distributions: a review and prospectus for future research. *Wiley Interdisciplinary Reviews: Water* **4**, e122x5. DOI: 10.1002/wat2.1225.

Li, X. Y., Hu, X., Zhang, Z. H., Peng, H. Y., Zhang, S. Y., Li, G. Y., Li, L. & Ma, Y. J. 2013 Shrub hydropedology: preferential water availability to deep soil layer. *Vadose Zone Journal* **12** (4). DOI: 10.2136/vzj2013.01.0006.

Liu, W., Luo, Q., Li, J., Wang, P., Lu, H., Liu, W. & Li, H. 2015 The effects of conversion of tropical rainforest to rubber plantation on splash erosion in Xishuangbanna, SW China. *Hydrology Research* **46** (1), 168–174. DOI: 10.2166/nh.2013.109.

Liu, J., Liu, W. & Zhu, K. 2018 Throughfall kinetic energy and its spatial characteristics under rubber-based agroforestry systems. *Catena* **161**, 113–121. DOI: 10.1016/j.catena.2017.10.014.

Llorens, P. & Gallart, F. 2000 A simplified method for forest water storage capacity measurement. *Journal of Hydrology* **240** (1), 131–144. DOI: 10.1016/S0022-1694(00)00339-5.

Loustau, D., Berbigier, P., Granier, A. & Moussa, F. E. H. 1992 Interception loss, throughfall and stemflow in a maritemporal pine stand. I. Variability of throughfall and stemflow beneath the pine canopy. *Journal of Hydrology* **138** (3–4), 449–467. DOI: 10.1016/0022-1694(92)90130-N.

Mizugaki, S., Nanko, K., Onda, Y., Tsujimura, M. & Yamashiki, Y. 2010 The effect of slope angle on splash detachment in an unmanaged Japanese cypress plantation forest. *Hydrological Processes* **24** (5), 576–587. DOI: 10.1002/hyp.7552.

Möttönen, M., Järvinen, E., Hokkanen, T. J., Kuuluvainen, T. & Ohtonen, R. 1999 Spatial distribution of soil ergosterol in the organic layer of a mature Scots pine (Pinus sylvestris L.) forest. *Soil Biology and Biochemistry* **31** (4), 503–516. DOI: 10.1016/S0038-0717(98)00122-9.

Nanko, K., Onda, Y., Ito, A., Ito, S., Mizugaki, S. & Moriwaki, H. 2010 Variability of surface runoff generation and infiltration rate under a tree canopy: indoor rainfall experiment using Japanese cypress (*Chamaecyparis obtusa*). *Hydrological Processes* **24** (5), 567–575. DOI: 10.1002/hyp.7551.

Nanko, K., Onda, Y., Kato, H. & Gomi, T. 2016 Immediate change in throughfall spatial distribution and canopy water balance after heavy thinning in a dense mature Japanese cypress plantation. *Ecohydrology* **9** (2), 300–314. DOI: 10.1002/eco.1636.

Návar, J., González, J. M. & Gonzalez, H. 2009 Gross precipitation and throughfall chemistry in legume species planted in Northeastern México. *Plant and Soil* **318** (1–2), 15–26. DOI: 10.1007/s11104-008-9812-0.

Raat, K., Draaijers, G., Schaap, M., Tietema, A. & Verstraten, J. 2002 Spatial variability of throughfall water and chemistry and forest floor water content in a Douglas fir forest stand. *Hydrology and Earth System Sciences Discussions* **6** (3), 363–374. DOI: 10.5194/hess-6-363-2002.

Rosier, C. L., Van Stan, J. T., Moore, L. D., Schrom, J. O., Wu, T., Reichard, J. S. & Kan, J. 2015 Forest canopy structural controls over throughfall affect soil microbial community structure in an epiphyte-laden maritemporal oak stand. *Ecohydrology* **8** (8), 1459–1470. DOI: 10.1002/eco.1595.

Shachnovich, Y., Berliner, P. R. & Bar, P. 2008 Rainfall interception and spatial distribution of throughfall in a pine forest planted in an arid zone. *Journal of Hydrology* **349** (1–2), 168–177. DOI: 10.1016/j.jhydrol.2007.10.051.

Shen, H., Wang, X., Jiang, Y. & You, W. 2012 Spatial variations of throughfall through secondary succession of evergreen broad-leaved forests in eastern China. *Hydrological Processes* **26** (11), 1739–1747. DOI: 10.1002/hyp.8251.

Shi, Z. J., Wang, Y. H., Xiong, W., Yu, P. T., Guo, H., Zhang, L. Y. & Dong, H. X. 2006 The spatial heterogeneity of throughfall under Larix principis-rupprechtii single tree's canopy. *Acta Ecologica Sinica* **26** (9), 2877–2886 (in Chinese with English abstract). DOI:10.3321/j.issn:1000-0933.2006.09.013.

Staelens, J., De Schrijver, A., Verheyen, K. & Verhoest, N. E. 2006 Spatial variability and temporal stability of throughfall water under a dominant beech (Fagus sylvatica L.) tree in relationship to canopy cover. *Journal of Hydrology* **330** (3), 651–662. DOI: 10.1016/j.jhydrol.2006.04.032.

Sun, X., Onda, Y., Chiara, S., Kato, H. & Gomi, T. 2015 The effect of strip thinning on spatial and temporal variability of throughfall in a Japanese cypress plantation. *Hydrological Processes* **29** (24), 5058–5070. DOI: 10.1002/hyp.10425.

Tanaka, N., Levia, D., Igarashi, Y., Nanko, K., Yoshifuji, N., Tanaka, K., Tantasirin, C., Suzuki, M. & Kumagai, T. 2015 Throughfall under a teak plantation in Thailand: a multifactorial analysis on the effects of canopy phenology and meteorological conditions. *International Journal of Biometeorology* **59** (9), 1145–1156. DOI: 10.1007/s00484-014-0926-1.

Teale, N. G., Mahan, H., Bleakney, S., Berger, A., Shibley, N., Frauenfeld, O. W., Quiring, S. M., Rapp, A. D., Roark, E. B. & Washington-Allen, R. 2014 Impacts of vegetation and precipitation on throughfall heterogeneity in a tropical pre-montane transitional cloud forest. *Biotropica* **46** (6), 667–676. DOI: 10.1111/btp.12166.

Vega, J., Fernández, C. & Fonturbel, T. 2005 Throughfall, runoff and soil erosion after prescribed burning in gorse shrubland in Galicia (NW Spain). *Land Degradation & Development* **16** (1), 37–51. DOI: 10.1002/ldr.643.

Wullaert, H., Pohlert, T., Boy, J., Valarezo, C. & Wilcke, W. 2009 Spatial throughfall heterogeneity in a montane rain forest in Ecuador: extent, temporal stability and drivers. *Journal of Hydrology* **377** (1), 71–79. DOI: 10.1016/j.jhydrol.2009.08.001.

Zhang, K. 1988 The climatic dividing line between SW and SE monsoons and their differences in climatology and ecology in Yunnan Province of China. *Climatological Notes* **38**, 197–207.

Zhang, Y. F., Wang, X. P., Hu, R. & Pan, Y. X. 2016 Throughfall and its spatial variability beneath xerophytic shrub canopies within water-limited arid desert ecosystems. *Journal of Hydrology* **539**, 406–416. DOI: 10.1016/j.jhydrol.2016.05.051.

Zimmermann, A., Wilcke, W. & Elsenbeer, H. 2007 Spatial and temporal patterns of throughfall quantity and quality in a tropical montane forest in Ecuador. *Journal of Hydrology* **343** (1–2), 80–96. DOI: 10.1016/j.jhydrol.2007.06.012.

Zimmermann, A., Zimmermann, B. & Elsenbeer, H. 2010 Comment on 'Spatial throughfall heterogeneity in a montane rain forest in Ecuador: extent, temporal stability and drivers' by Wullaert *et al.* [Journal of Hydrology, 377(2009): 71–79]. *Journal of Hydrology* **395** (1), 133–136. DOI: 10.1016/j.jhydrol.2010.10.013.

First received 8 February 2018; accepted in revised form 19 July 2018. Available online 6 August 2018